Article

Not peer-reviewed version

Impact of Oncogenic Changes in p53 and KRAS on Macropinocytosis and Ferroptosis in Colon Cancer Cells and Anticancer Efficacy of Niclosamide with Differential Effects on These Two Processes

Nhi T. Nguyen , Souad R. Sennoune , Gunadharini Dharmalingam-Nandagopal , Sathish Sivaprakasam , Yangzom D. Bhutia , Vadivel Ganapathy *

Posted Date: 4 April 2024

doi: 10.20944/preprints202404.0092.v2

Keywords: p53 loss; KRAS mutation; SLC7A11; SLC38A5; ferroptosis; macropinocytosis; antioxidant machinery; lipid peroxidation; niclosamide; colon cancer

Article

Impact of Oncogenic Changes in p53 and KRAS on Macropinocytosis and Ferroptosis in Colon Cancer Cells and Anticancer Efficacy of Niclosamide with Differential Effects on these Two Processes

Nhi T. Nguyen, Souad R. Sennoune, Gunadharini Dharmalingam-Nandagopal, Sathish Sivaprakasam, Yangzom D. Bhutia and Vadivel Ganapathy *

Department of Cell Biology and Biochemistry, Texas Tech University Health Sciences Center, Lubbock, TX 79430, USA; Nhi.T.Nguyen@ttuhsc.edu; Souad.Sennoune@ttuhsc.edu; gnandago@ttuhsc.edu; Sathish.sivaprakasam@ttuhsc.edu; yangzom.d.bhutia@ttuhsc.edu; vadivel.ganapathy@ttuhsc.edu

* Correspondence: vadivel.ganapathy@ttuhsc.edu

Abstract: Mutations in p53 and KRAS are seen in most cases of colon cancer. The impact of these mutations on signaling pathways related to cancer growth has been studied in depth, but relatively less is known on their effects on amino acid transporters in cancer cells. This represents a significant knowledge gap because amino acid nutrition in cancer cells profoundly influences macropinocytosis and ferroptosis, two processes with opposing effects on tumor growth. Here we used isogenic colon cancer cell lines to investigate the effects of p53 loss and KRAS activation on two amino acid transporters relevant to macropinocytosis (SLC38A5) and ferroptosis (SLC7A11). Our studies show that the predominant effect of p53 loss is to induce SLC7A11 with resultant potentiation of antioxidant machinery and protection of cancer cells from ferroptosis whereas KRAS activation induces not only SLC7A11 but also SLC38A5, thus offering protection from ferroptosis as well as improving amino acid nutrition in cancer cells via accelerated macropinocytosis. Niclosamide, an FDA-approved anti-helminthic, blocks the functions of SLC7A11 and SLC38A5, thus inducing ferroptosis and suppressing macropinocytosis with resultant effective reversal of tumor-promoting actions of oncogenic mutations in p53 and KRAS. These findings underscore the potential of this drug in colon cancer treatment.

Keywords: p53 loss; KRAS mutation; SLC7A11; SLC38A5; ferroptosis; macropinocytosis; antioxidant machinery; lipid peroxidation; niclosamide; colon cancer

1. Introduction

As per the most recent colorectal cancer statistics-2023, colorectal cancer is the third most commonly diagnosed cancer in both men and women in the United States [1–3]. It is also the cause of second most cancer-related deaths in men and the most prominent cancer-related death in younger men (<50 years of age). It was estimated that more than 150,000 new cases of cancer in colon/rectum would have been diagnosed in year 2023 [1–3]. Colorectal cancer is the cause of approximately one million deaths worldwide every year. There are several risk factors for colorectal cancer, including age, sex, family history, diet, inflammation, and gene mutations. Truly alarming is the estimate that about 4% of men and women will be diagnosed with colorectal cancer at some point in their lifetime [2]. Due to increased implementation of routine screening procedures and resultant early detection and also due to newly developed drugs for effective treatment, the 5-year survival in patients with colorectal cancer has been steadily increasing over the years, from about 50% in 1975 to about 70% in 2015 in most countries, including the United States [4].

Several germline and somatic mutations are associated with colorectal cancer [5–7]. These mutations occur in tumor suppressor genes, oncogenes, and DNA repair genes. A small percentage

 doi:10.20944/preprints202404.0092.v2

of colorectal cancer is inheritable where germline mutations are found in the genes coding for the adenomatous polyposis coli (APC) (Gardner syndrome), the tumor suppressor LKB1 (Peutz-Jeghers syndrome), DNA repair proteins MLH1, MSH2, MSH6, PMS2, EPCAM, and MUTYH (Lynch syndrome), and cystic fibrosis transmembrane conductance regulator CFTR (cystic fibrosis) [5–7]. Most cases of colorectal cancer are sporadic, and somatic mutations underlie carcinogenesis in these cases. Most often, mutations in APC with resultant activation of β-catenin-dependent signaling and transcription initiate rapid cell proliferation, followed by mutations in the oncogene KRAS and subsequently in the tumor suppressor p53 that mediate and maintain cellular transformation and cancer growth [8–10]. APC is an integral part of the destruction complex that promotes proteasomal degradation of β-catenin; therefore, loss-of-function mutations in APC, which prevent β-catenin degradation, are associated with colorectal cancer. Mutations in KRAS related to colorectal cancer result in gain-of-function with a decrease in GTPase activity of RAS and hence an increase in GTP-bound RAS and consequent persistent activation of signaling pathways responsible for cell proliferation and carcinogenic cellular transformation. Mutations in p53 found in colorectal cancer interfere with the transcriptional activity of the protein, thus protecting the cells from apoptosis and promoting cell proliferation and growth.

Macropinocytosis and ferroptosis are two biological phenomena that have come to the forefront in the field of cancer biology in relatively more recent years. Both these processes are connected to cancer-cell nutrition: macropinocytosis to amino acid nutrition [11,12] and ferroptosis to iron/amino acid nutrition [13,14]. Oncogenic mutations in KRAS are associated with induction of macropinocytosis that mediate the uptake of extracellular proteins for subsequent hydrolysis when macropinosomes fuse with lysosomes followed by the use of the resultant amino acids in cellular metabolism. Tumor-associated blood vessels are often leaky [15,16], thus facilitating the release of plasma proteins such as albumin into the extracellular milieu that are used in macropinocytosis. Even though the incidence of KRAS mutations is significant in colorectal cancer (30-50%), it occurs far more frequently in pancreatic cancer (~90%) [17]. As such, the association between KRAS mutations and macropinocytosis has been investigated mostly in relation to pancreatic cancer [11,12]. Macropinocytosis offers a novel mechanism for acquisition of amino acids in cancer cells in addition to the import of extracellular amino acids via multiple amino acid transporters that are upregulated in cancer [18–20]. As such, macropinocytosis promotes cancer by supplying amino acids to support cell proliferation. Cancer cells are also obligatorily dependent on iron for growth and proliferation [21,22], but excess iron increases the risk for iron-induced cell death ferroptosis. Cancer cells find ways to evade this form of cell death by potentiating glutathione-dependent antioxidant machinery. Loss-of-function mutations in p53 play an important role in this process where loss of p53 function leads to induction of the cystine transporter SLC7A11 to promote the synthesis of the antioxidant peptide glutathione in cancer cells [23,24]. In the current study, we focused on the relative importance of an oncogenic mutation in KRAS (G12D) and loss of p53 in macropinocytosis and ferroptosis in colon cancer using isogenic cancer cell lines with and without the KRAS mutation as well as with and without p53.

Current treatment options for colorectal cancer include removal of the cancerous tissue (surgery, radiofrequency ablation, and cryosurgery), radiation therapy, chemotherapy, and immunotherapy [25]. Monoclonal antibodies that neutralize the functions of VEGFRs and EGFRs on tumor cells and CTLA4 and PD-1 on cytotoxic T cells are increasingly used. Chemotherapy includes 5-fluorouracil and 5-trifluoro-2-deoxythymidine (inhibitors of thymidylate synthetase), irinotecan (an inhibitor of topoisomerase I), oxaliplatin (a DNA-alkylating agent that interferes with DNA replication and transcription), and several small-molecule inhibitors of the tyrosine kinase activity associated with VEGFRs and EGFRs [26]. However, none of these therapies specifically target macropinocytosis and/or ferroptosis in cancer cells. In the present study, we have identified niclosamide, an FDA-approved anti-helminthic drug [27,28], as not only a potent inhibitor of macropinocytosis but also an inducer of ferroptosis in colon cancer cells, thus underscoring the potential of this drug as an anticancer agent, especially for cancers associated with oncogenic changes in KRAS and p53.

 doi:10.20944/preprints202404.0092.v2

2. Materials and Methods

2.1. Materials

[2,3-^{3}H]-L-Serine (sp. radioactivity, 15 Ci/mmol) was purchased from Moravek, Inc. (Brea, CA, USA). [^{3}H]-Glutamate (sp. radioactivity, 50.8 Ci/mmol) was purchased from PerkinElmer Corp (Waltham, MA, USA). Niclosamide was from Millipore-Sigma (St. Louis, MO, USA) and ferrostatin-1 was from Santa Cruz Biotechnology Inc., (Dallas, TX, USA). All other chemicals were from Millipore-Sigma (St. Louis, MO, USA).

2.2. Cell Lines and Culture Conditions

We used two pairs of isogenic human colon cancer cell lines: HCT-116/*p53*$^{+/+}$ and HCT116/*p53*$^{-/-}$ cells (kindly provided by Dr. Bert Vogelstein (Johns Hopkins University School of Medicine, Baltimore, MD, USA) and SW48 parent and KRAS^{G12D} mutant cells (purchased from Horizon Discovery Ltd., Cambridge, UK). Additional relevant genotype features of these cell lines are given in the Results section. SW48 cells were cultured in RPMI 1640 medium, supplemented with 2 mM L-glutamine and 25 mM sodium bicarbonate. HCT-116 cells were cultured in McCoY's 5a medium. All media contained 10% fetal bovine serum. Cell cultures were tested every month for mycoplasma using a commercially available detection kit (cat. no. G238; Applied Biological Materials, Inc. Richmond, BC, Canada). All cell lines used in the present study were mycoplasma-free.

2.3. Uptake Measurement

Uptake of radiolabeled serine was used to monitor the transport function of SLC38A5. Since SLC38A5 is Na^+-coupled with H^+ movement in the opposite direction, the uptake assay was done at pH 8.5 to create an outward-directed H^+-gradient across the plasma membrane. As there are several Na^+-coupled transporters for serine, we cannot specifically monitor the function of SLC38A5 by using Na^+-buffer. However, unlike other Na^+-coupled transporters, SLC38A5 is tolerant to Li^+ (i.e., SLC38A5 is functional when Na^+ is replaced with Li^+). Therefore, we used an uptake buffer with LiCl in place of NaCl. The composition of the uptake buffer was 25 mM Tris/Hepes, pH 8.5, containing 140 mM LiCl, 5.4 mM KCl, 1.8 mM $CaCl_2$, 0.8 mM $MgSO_4$ and 5 mM glucose. Serine is also a substrate for SLC7A5, which is a Na^+-independent transporter; therefore, uptake via this transporter will contribute to the total uptake measured in the Li^+-buffer. Therefore, the uptake buffer contained 5 mM tryptophan to compete with and block SLC7A5-mediated serine uptake; SLC38A5 does not transport tryptophan and therefore SLC38A5-mediated serine uptake is not affected by tryptophan. To determine the contribution of diffusion to the total uptake of serine, the same uptake buffer but with LiCl replaced isosmotically with *N*-methyl-D-glucamine chloride (NMDGCl) was used. The uptake was measured in two buffers: (i) LiCl-buffer, pH 8.5 with 5 mM tryptophan; (ii) NMDGCl-buffer, pH 8.5 with 5 mM tryptophan. The uptake in NMDGCl-buffer was subtracted from the uptake in LiCl-buffer to determine the transport activity of SLC38A5 [29].

SLC7A11 is a Na^+-independent transporter that mediates the cellular entry of cystine in exchange for intracellular glutamate under physiological conditions. However, we routinely measure its transport function by cellular uptake of radiolabeled glutamate. Under these conditions, SLC7A11 mediates the cellular entry of radiolabeled glutamate in exchange for intracellular unlabeled glutamate. Transport activity was measured using a Na^+-free buffer (25 mM Hepes/Tris, 140 mM *N*-methyl-D-glucamine chloride, 5.4 mM KCl, 1.8 mM $CaCl_2$, 0.8 mM $MgSO_4$, and 5 mM glucose, pH 7.5). The diffusional component was determined by measuring the uptake of radiolabeled glutamate in the presence of excess unlabeled glutamate (5 mM). The transport activity of SLC7A11 was calculated by subtracting the diffusional component from total uptake [30].

Cells were seeded in 24-well culture plates (2×10^5 cells/well) and allowed to grow to confluency, which normally took 2 or 3 days depending on the cell line. On the day of uptake measurement, the culture plates were kept in a water bath at 37 °C. The medium was aspirated, and the cells were washed with uptake buffers. The uptake medium (250 µl) containing corresponding amino acid as the tracer was added to the cells. Following incubation for 15 min (SLC38A5) or 30 min (SLC7A11),

 doi:10.20944/preprints202404.0092.v2

the medium was removed, and the cells were washed thrice with ice-cold uptake buffer. The cells were then lysed in 1% sodium dodecyl sulfate/0.2 N NaOH and used for measurement of radioactivity.

2.4. Intracellular pH Measurement

The methodology used to monitor intracellular pH has been described previously [29]. Cells were grown on rectangular coverslips (9 × 22 mm) until they became confluent. These cells were then incubated with 7.5 μM SNARF-1-AM in the perifusion buffer at an extracellular pH of 7.4 for 30 min at 37 ’C, followed by a 30-min incubation in the same buffer but without the dye. This allows hydrolysis of the SNARF-1-AM ester within the cells. Two coverslips were placed back-to-back (cells facing outside) in a holder and perifused at a rate of 3 ml/min, and the fluorescence of SNARF-1 was monitored with a SLC-8100/DMX spectrofluorometer (Spectronics Instruments, Rochester, NY, USA). In situ calibration curves were generated as follows. The cells on coverslips were perifused with a high K^+-buffer (10 mM NaCl, 146 mM KCl, 10 mM HEPES, 10 mM MES, 10 mM Bicine, 2 μM valinomycin, 6.8 μM nigericin, 5 mM glucose, pH 5.5–8.0 at 0.2 pH intervals). The 644 nm/584 nm ratio of SNARF-1 fluorescence was determined at each pH and then converted to pH using a modified Henderson–Hasselbalch equation. This calibration was used to calculate intracellular pH in control cells and in cells exposed to niclosamide.

2.5. Macropinocytosis Assay

We used TMR (tetramethylrhodamine)-dextran (molecular weight, 70 kDa) as a probe to monitor macropinocytosis as described by others [31,32] and in our previous publication [29]. Briefly, cells were plated on coverslips, placed in wells in a 12-well plate, at a density of 1×10^5 cells/well, and cultured at 37 ’C using the culture media recommended for the cells. The cells were allowed to reach ~70% confluency. Cells were washed thrice with a buffer consisting of 140 mM NaCl, 5.4 mM KCl, 1.8 mM $CaCl_2$, 0.8 mM $MgSO_4$, and 5 mM glucose, pH 7.5. Subsequently, the cells were exposed to TMR-dextran (100 μg/ml) in the same buffer at 37 °C. Then, the cells were washed thrice with the respective buffer and then fixed with 4% paraformaldehyde for 5 min, washed several times with phosphate-buffered saline, and mounted using Prolong diamond with 4,6-diamidino-2-phenylindole (DAPI) as a nuclear marker. Cell images were taken using a Nikon T1-E microscope with A1 confocal super-resolution module (Nikon, Dallas, TX, USA) with a 60× objective. The fluorescence quantification was performed by measuring the corrected total cell fluorescence (CTCF) using Image J and the following formula:

CTCF = (integrated density) − (area of cell of interest) × (mean fluorescence of background).

For groups of cells (15–20 cells/field) in an image, an outline was drawn to measure integrated density, area of the cells of interest, and mean fluorescence of the adjacent background around the cells of interest. We randomly selected five separate fields with 15–20 cells and calculated CTCF for each field; the five CTCF values were averaged.

2.6. RT-PCR

Total RNA was extracted from cells using TRIzol Reagent (Thermo Fisher Scientific, Waltham, MA, USA), and the RNA was reverse-transcribed using a high-capacity cDNA reverse transcription kit (Thermo Fisher Scientific, Waltham, MA, USA). Quantitative PCR were performed with Power SYBR Green PCR master mix (Bio-Rad, Hercules, CA, USA). Primer sequences are given in supplemental Table S1. The relative mRNA expression was determined by the $2^{-\Delta\Delta Ct}$ method with 18S mRNA for normalization.

2.7. Protein Isolation and Western Blot

Cells were lysed in Pierce™ RIPA buffer (Thermo Fisher Scientific, Waltham, MA, USA) supplemented with Halt™ Protease and Phosphatase Inhibitor Cocktail (Thermo Fisher Scientific, Waltham, MA, USA). Protein was measured using Pierce™ BCA Protein Assay Kit (Thermo Fisher

 doi:10.20944/preprints202404.0092.v2

Scientific, Waltham, MA, USA). The samples, prepared in Laemmli Sample Buffer (Bio-Rad Labs, Hercules, CA, USA), were loaded onto a SDS–PAGE gel and transferred onto a PVDF membrane. The membrane was blocked, and antibodies diluted in 5% nonfat dry milk. Protein bands were visualized using Pierce™ ECL Western Blotting Substrate (Thermo Fisher Scientific, Waltham, MA, USA) and developed on an autoradiography film. Most primary antibodies were purchased from Cell Signaling Technology (Danvers, MA, USA): FTH (#4393), GPX4 (#52455), HSP60 (#12165), SLC7A11 (#12691), and SLC3A2 (#47213). Antibodies for p53 (#SC-126) and Myc (#SC-40) were from Santacruz Biotechnology (Dallas, TX, USA). Secondary antibody horseradish peroxidase-conjugated goat anti-rabbit (#1706515) was from Bio-Rad Labs (Hercules, CA, USA). For quantification of protein levels by densitometry, the experiment was done in triplicate.

2.8. Assays for Lipid Radicals (Ferroptosis) and Iron

Lipid radical (ferroptosis) assay and iron assay were done as originally described by others [33,34] and used in one of our previous publications [30]. Cells were cultured on a 25-mm glass coverslip to ~70% confluency. Cells were washed with NaCl buffer, pH 7.5 and then incubated with 1 μM of LipiRadical Green (FDV-0042, Funakoshi, Tokyo, Japan) or Ferro-orange (F374, Dojindo, Rockville, MD, USA) in NaCl buffer, pH 7.5 for 20 min and then washed. To analyze the effect of niclosamide on lipid peroxidation, the cells were treated with the fluorescent probe along with niclosamide for 20 min and then washed. The glass coverslip containing the cells was then probed under an inverted microscope. The fluorescence imaging was captured using a Nikon T1-E microscope with A1 confocal super-resolution module (Nikon, Dallas, TX, USA), with a 60× objective. For ferroptosis assay, the excitation was at 470 nm and the emission was at 520 nm; for iron assay, the excitation was at 560 nm and the emission was at 620 nm. The images represent a maximum projection intensity derived from a Z-stack. The fluorescence quantification was performed by measuring the corrected total cell fluorescence (CTCF) using Image J (version: 2.14.0/1.54f) and the following formula; CTCF = (integrated density) − (area of cell of interest) × (mean fluorescence of background).

2.9. Glutathione and Lipid Peroxidation Assay

Control and niclosamide-treated cells were used to measure glutathione levels (GSH-Glo assay, Promega, Madison, WI, USA). Malondialdehyde (MDA), a lipid peroxidation product, was measured using lipid peroxidation kit (MAK085, Millipore-Sigma, St. Louis, MO, USA).

2.10. Colony-Formation Assay

Colony-formation (clonogenic) assay was carried out with different doses of niclosamide. Initial seeding was 500 cells/well and culture was continued for 10 days with culture medium replaced with fresh medium every other day. At the end of the 10-day period, the medium was removed, and the colonies were fixed with ice-cold methanol/acetone and then stained with Giemsa stain. After examination, lysis buffer added (1% sodium dodecyl sulfate/0.2 N NaOH) and the extracted chromophore was quantified using Microplate Reader (Glomax multi-detection system, Promega, Madison, WI, USA).

2.11. MTT Assay

MTT assay was used to assess metabolic activity in cells, a substitute for cell vaibility and proliferation. This involves NAD(P)H-dependent reduction of the tetrazolium dye MTT, which is 3-(4,5-dimethylthiazol-2-yl)-2,5-diphenyltetrazolium bromide. Cells were seeded in 96-well plates and cultured for 24 h after which cells were exposed to niclosamide. Cells were cultured for an additional 72 h with fresh medium supplied every 24 h. Cells were then washed with phosphate-buffered saline twice followed by MTT reagent (ATCC, Manassas, VA, USA). Treatment and lysis of the cells were done as per the manufacturer's instructions. Absorbance of the lysate was measured at 550 nm.

 doi:10.20944/preprints202404.0092.v2

2.12. Chromatin-Immunoprecipitation (ChIP) Assay

ChIP assays were performed using EZ-Magna ChIP A/G kit (Millipore, Burlington, MA, USA). SW48 cells were treated with 1% formaldehyde for 10 min to crosslink proteins and nucleic acids. The contents were then collected in phosphate-buffered saline, supplemented with Halt™ Protease and Phosphatase Inhibitor Cocktail (Thermo Fisher Scientific, Waltham, MA, USA) and lysed in nuclear lysis buffer. The lysate was then sonicated using BioRuptor Plus (Diagenode, Denville, NJ, USA) to shear DNA into fragments of approximately 200–1,000 base-pairs. DNA concentration was measured using NanoDrop Spectrophotometer (Thermo Fisher Scientific, Waltham, MA, USA) and 100 μg of DNA was used for immunoprecipitation with anti-p53 (#SC-126) and anti-Myc (#SC-40) antibodies (Santacruz Biotechnology, Dallas, TX, USA), or normal mouse IgG (Millipore-Sigma, St. Louis, MO, USA). Before immunoprecipitation, a small aliquot of the supernatant was removed for use as an input. Immunoprecipitated DNA was isolated on the column and relative enrichment of p53 and Myc on SLC38A5 promoter was assessed via PCR. The PCR primer sequences are provided in Supplemental Table S1.

2.13. Assay for Reactive Oxygen Species (ROS) with 2',7'-Dichlorodihydrofluorescein Diacetate Staining

The fluorecent probe of DCFH-DA was used to measure ROS [35]. Briefly, cells were grown in a 96-well plate and then incubated with DCFH-DA (10 μM) at 37 °C for 30 min in dark. At the end of the incubation, cells were treated with different concentrations of niclosamide. Fluorescence intensity was monitored with a Microplate Reader (Glomax multi-detection system, Promega, Madison, WI, USA) at the excitation and emission wavelengths of 485 and 528 nm, respectively. Cellular fluorescence levels were expressed as per ug of protein.

2.14. Statistics

Uptake experiments were routinely done in triplicates, and each experiment was repeated at least thrice using independent cell cultures. Statistical analysis was performed with a two- tailed, paired Student's t-test for single comparison and a p-value <0.05 was considered statistically significant. Data are given as means ± S.E. For quantification of fluorescence signals related to macropinocytosis and ferroptosis, ANOVA followed by Dunn's test was used to determine the significance of difference among different groups.

3. Results

3.1. Origin and Genetic Background of Colon Cancer Cell Lines Used in This Study

Two pairs of isogenic human colon cancer cell lines were used in this study. The parent HCT-116 cell line was originally derived from colorectal adenocarcinoma in a 48-year-old male. This cell line possesses wild type APC and wild type p53, but mutant β-catenin where the mutation stabilizes the protein, thus leading to persistent transcriptional activity of β-catenin. KRAS in this cell line harbors the oncogenic mutation G13D. PTEN and BRAF are wild type in this cell line *[36–40]*. This cell line was used to generate a p53-null cell line in the laboratory of Dr. Vogelstein (Johns Hopkins University School of Medicine, Baltimore, MD, USA). The parent SW48 cell line was originally derived from colorectal adenocarcinoma in a 83-year-old female. This cell line possesses wild type APC, KRAS, p53, PTEN, and BRAF, but mutant β-catenin that stabilizes the protein with resultant persistent transcriptional activity *[36–40]*. This cell line was used to generate a KRAS mutant (G12D) cell line by Horizon Discovery Ltd. (Cambridge, UK). The status of APC, KRAS and p53 in these two pairs of isogenic cell lines, which are direclty relevant to the present study, are given in Table 1.

Table 1. Genetic background of the four human colon cancer cell lines used in the study.

Gene/Cell Line	HCT-116	HCT-116/p53 KO	SW48	SW48/KRAS mutant
APC	Wild type	Wild type	Wild type	Wild type

 doi:10.20944/preprints202404.0092.v2

KRAS	pGly13Asp (G13D)	pGly13Asp (G13D)	Wild type	pGly12Asp (G12D)
TP53 (p53)	Wild type	Deleted	Wild type	Wild type

As such, when macropinocytosis and ferroptosis and their associated cellular pathways are compared between the isogenic cell lines HCT-116 and HCT-116/p53 KO, the observed differences are most likely due to the presence or absence of functional p53 in a colon cancer cell line on the background of an oncogenic KRAS mutation and an active β-catenin signaling pathway. Similarly, when the isogenic cell lines SW48 and SW48/KRAS mutant are used for comparison, the observed differences are most likely due to the presence or absence of an oncogenic mutation in KRAS in a colon cancer cell line on the background of functional p53 and an active β-catenin signaling pathway.

3.2. Impact of p53 Loss and KRAS-G12D on SLC38A5 Expression and Function

Several studies have demonstrated the involvement of Na^+/H^+ exchanger in macropinocytosis [41,42]. Here the exchanger-mediated alkalinization of the cytoplasmic domain of the plasma membrane influences submembranous reorganization of actin cytoskeleton to form membrane ruffles that might promote invagination and closure of the plasma membrane to form macropinosomes, a non-clathrin/non-receptor-mediated endocytic process. Recently, we found that the amino acid transporter SLC38A5, which functions as an amino acid-dependent Na^+/H^+ exchanger, is also able to induce macropinocytosis in breast cancer cells [43]. SLC38A3, another amino acid transporter that functions similar to SLC38A5, may also affect macropinocytosis [44], but this has not yet been investigated experimentally. In the present study, we examined the influence of p53 and KRAS mutation on the expression and function of SLC38A3 and SLC38A5 by RT-PCR and transport function. Deletion of *p53* in HCT-116 cells decreased the transport function of SLC38A3/SLC38A5 significantly even though the steady-state levels of SLC38A3 mRNA and SLC38A5 mRNA appeared to be little affected (Figure 1A, B). In SW48 cells, the presence of the oncogenic mutation in KRAS (G12D) induced the expression (i.e., increase in mRNA levels) and function (i.e., transport activity) of both transporters (Figure 1A, B). The changes observed in Na^+-coupled serine uptake may not be entirely due to changes in SLC38A3/SLC38A5 expression, but the changes in Li^+-coupled serine uptake certainly are. Even though we were not able to differentiate between SLC38A3 and SLC38A5 in terms of Li^+-coupled serine uptake (no selective inhibitors available yet) in these cell lines, we believe that SLC38A5 is the predominant contributor to the observed uptake based on the relative levels of the respective mRNAs as determined from ΔCt values in qRT-PCR (ratio of SLC38A5 : SLC38A3 mRNA level was 8:1 in HCT-116 cells and 52:1 in SW48 cells). Based on these data, we conclude that even though p53 is a tumor suppressor whereas KRAS-G12D is an oncogenic mutation, both induce SLC38A5 expression.

 doi:10.20944/preprints202404.0092.v2

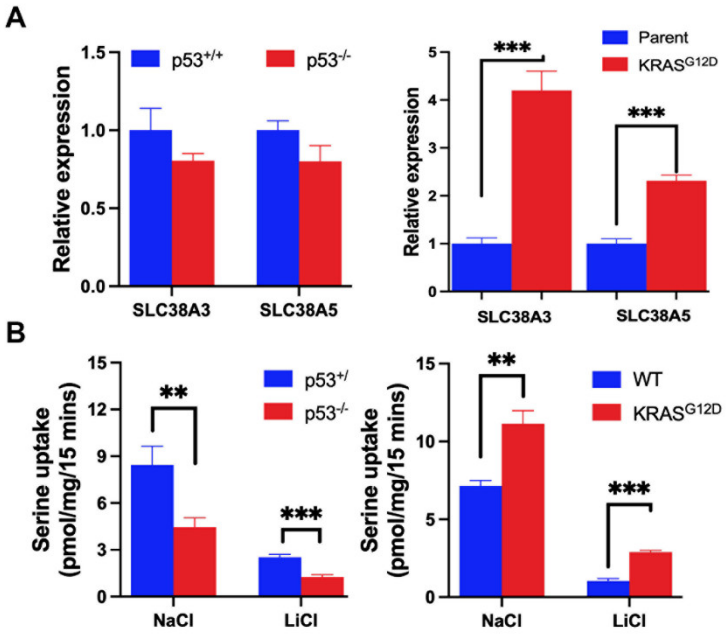

Figure 1. Expression and function of SLC38A3/SLC38A5 in the two pairs of isogenic colon cancer cell lines with and without p53 (HCT-116) and with and without G12D mutation in KRAS (SW48). Relative expression of mRNA levels as assessed by qRT-PCR (**A**). Transport function as assessed by serine uptake (**B**). Data are mean ± S.E. for three independent experiments. **, $p < 0.01$; ***, $p < 0.001$. When not specified, the difference is not statistically significant.

3.3. Interaction of p53 and Myc with SLC38A5 Promoter

The function of p53 as a transcription factor is well known. In contrast, the downstream pathway for RAS involves phosphorylation cascades [45,46]. The gene expression induced by RAS signaling is mediated by several transcription factors including Ets, Fos, Jun, and Myc [47,48]. Here we focused on Myc because of its role as an oncogene and also because of a previous report that SLC38A5 (identified as SN2 in the report) is induced in cancer cells upon ectopic expression of Myc [49]. Since our experiments showed that both p53 and KRAS mutant induce SLC38A5 expression, we performed ChIP to demonstrate the binding of p53 and Myc to SLC38A5 gene promoter. First, we analyzed the promoter sequence for p53- and Myc-binding sites using the eukaryotic promoter database (https://epd.expasy.org/epd), a webtool created and managed by the Computational Cancer Genomics (CCG) lab of the Swiss Institute of Bioinformatics (SIB). We found numerous binding motifs for both transcription factors in human SLC38A5 gene promoter (Figure 2A). We then monitored the protein levels for p53 and Myc in all four cell lines used in the study (Figure 2B). This experiment confirmed the absence of p53 in HCT-116/p53 KO cells. More importantly, Myc protein levels were higher in SW48/KRAS mutant cells than in parent SW48 cells. Interestingly, Myc levels were higher also in *p53*-null HCT-116 cells than in parent HCT-116 cells. The ChIP experiment demonstrated the binding of both p53 and Myc to the SLC38A5 promoter (Figure 2C). The observed increase in the expression of SLC38A5 in SW48/KRAS mutant cells agrees with the increased levels of Myc in these cells. In contrast, the observed decrease in the expression of SLC38A5 in *p53*-null HCT-116 cells in spite of the increase in Myc protein levels suggests a more predominant role for p53 than for Myc in the control of SLC38A5 expression in this particular cell line.

 doi:10.20944/preprints202404.0092.v2

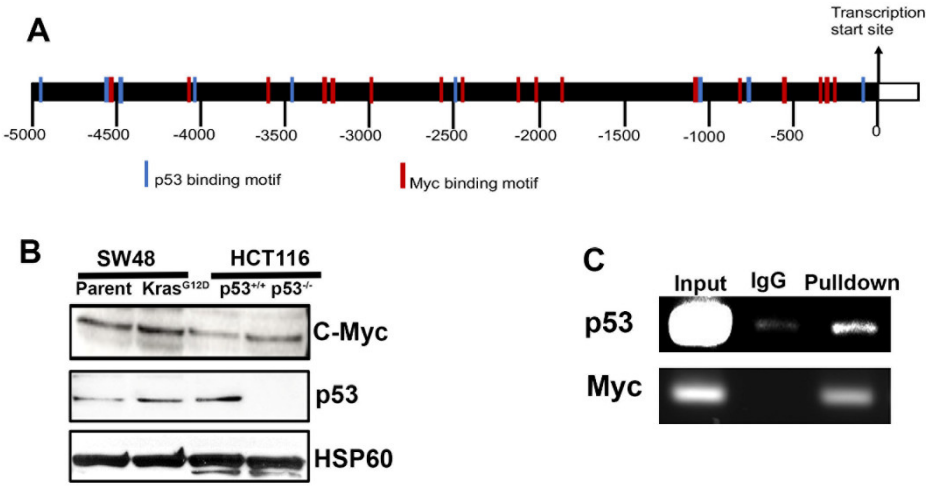

Figure 2. Evidence for SLC38A5 as a transcriptional target for p53 and Myc. Locations for theoretical binding sites in human SLC38A5 gene promoter for p53 and Myc (**A**). Protein levels for p53 and Myc in the isogenic cell lines SW48 with and without KRAS-G12D mutation and HCT-116 with and without p53 (**B**). SW48 parent cells were used for ChIP assay to provide evidence for the binding of p53 and Myc to the SLC38A5 gene promoter (**C**).

3.4. Impact of p53 and KRAS Mutation on Macropinocytosis

We monitored macropinocytosis using TMR-dextran in all four cell lines to determine how the deletion of p53 in HCT-116 cells and the presence of the oncogenic KRAS mutation G12D in SW48 cells affect this process (Figure 3). Macropinocytosis was robust in HCT-116 cells that already harbors the oncogenic mutation G13D in KRAS; deletion of p53 in this cell did not have any noticeable effect on macropinocytosis. In contrast, macropinocytosis was relatively lower in SW48 parent cells than in HCT-116 parent cells, and the presence of the oncogenic mutation G12D in KRAS in SW48 cells markedly increased macropinocytosis. Collectively, these findings show that the process of macropinocytosis in colon cancer cells is controlled by KRAS with little impact from p53.

 doi:10.20944/preprints202404.0092.v2

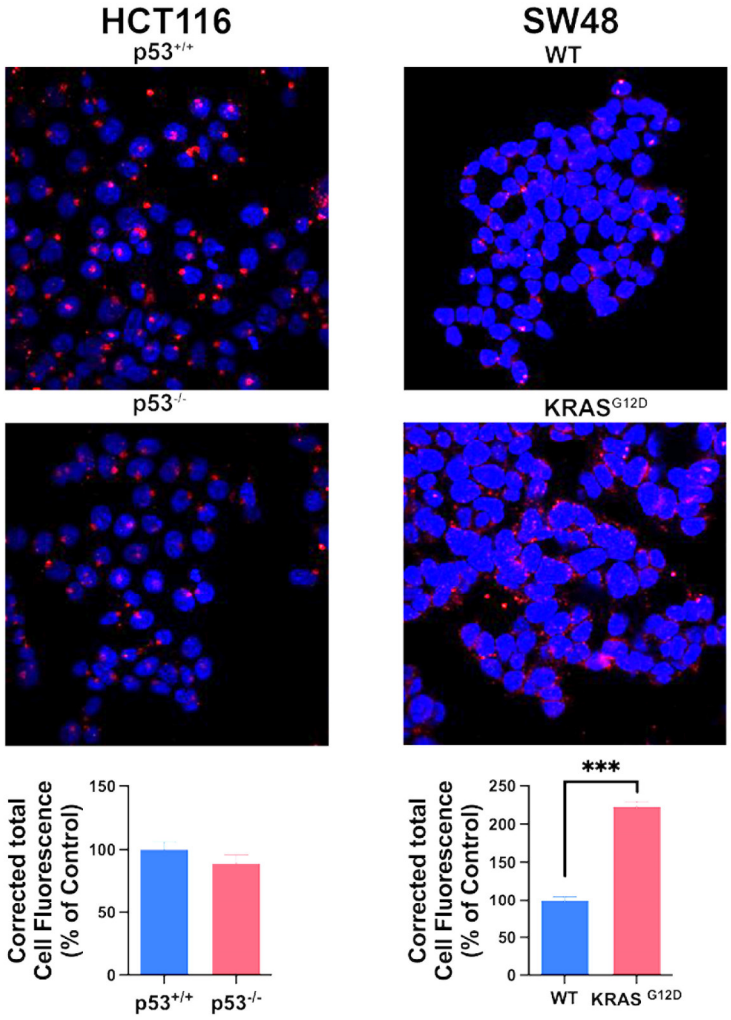

Figure 3. Effect of p53 loss and oncogenic KRAS mutation G12D on macropinocytosis. Cellular uptake of TMR-dextran was used to monitor macropinocytosis activity. The fluorescence signals were quantified as CTCF (corrected total cell fluorescence) for all four cell lines. Data are mean ± S.E. ***, $p < 0.001$. When not specified, the difference is not statistically significant.

3.5. Influence of p53 and KRAS Mutation on the Expression and Function of SLC7A11

The primary mechanism for the protection of cells from iron-induced cell death ferroptosis is glutathione, which removes lipid peroxides by the activity of glutathione peroxidase [50]. Accordingly, the amino acid transporter SLC7A11, which provides the limiting amino acid cysteine for glutathione synthesis, is an important controller of ferroptosis in cancer cells [51,52]. The recruitment of SLC7A11 to the plasma membrane requires a protein chaperone, called SLC3A2, and the functionally active complex is a heterodimer consisting of the chaperone SLC3A2 and the actual transporter SLC7A11 [53,54]. Therefore, we examined the expression of the transporter as well as the chaperone in the four cancer cell lines. We found the expression of both components of the transport system to be increased markedly by p53 loss and KRAS-G12D mutation (Figure 4A, B). This increase in mRNA levels corresponded to an increase in transport function as monitored by glutamate uptake (Figure 4C, D) and protein levels (Figure 4E, F). These data show that p53 is a suppressor of SLC7A11/SLC3A2 expression whereas the oncogenic mutation G12D in KRAS is an inducer. This is in contrast to the effects of p53 and KRAS mutation on SLC38A5 expression where both induce the expression.

 doi:10.20944/preprints202404.0092.v2

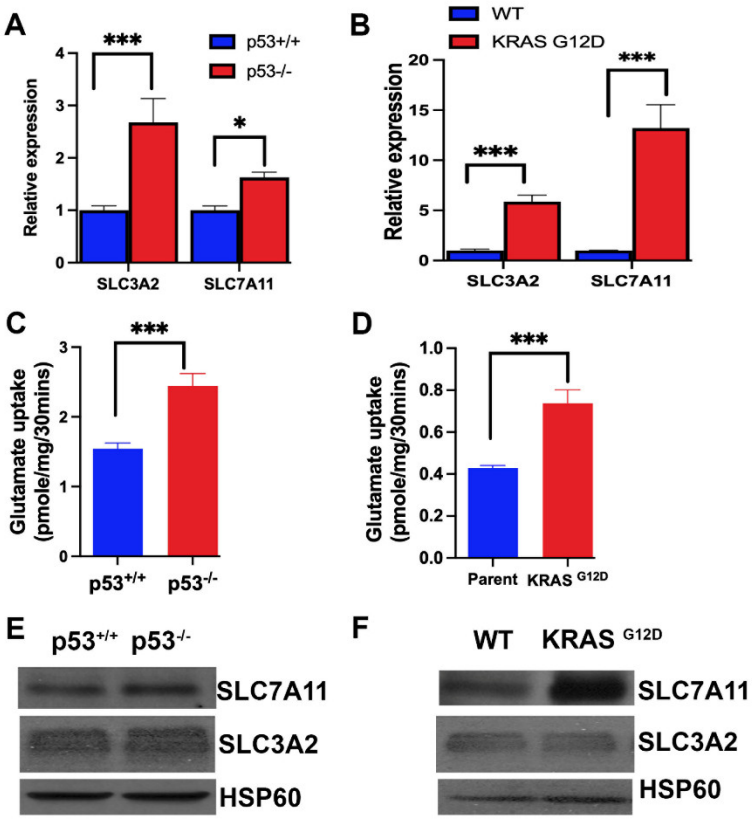

Figure 4. Expression and function of SLC7A11 (and its chaperone SLC3A2) in the two pairs of isogenic colon cancer cell lines with and without p53 (HCT-116) and with and without G12D mutation in KRAS (SW48). Relative expression of mRNA levels as assessed by qRT-PCR (**A**, **B**). Transport function as assessed by glutamate uptake (**C**, **D**). Data are mean ± S.E. for three independent experiments. *, $p < 0.05$; ***, $p < 0.001$. Protein levels for SLC7A11 and SLC3A2 in the four cell lines (**E**, **F**).

3.6. Impact of p53 Loss and KRAS-G12D Mutation on Ferroptosis

To determine the relative importance of p53 loss and the oncogenic mutation in KRAS in protection of colon cancer cells from ferroptosis, we monitored ferroptosis in all four cell lines using a fluorescence assay that is based on cellular levels of ferroptosis-inducing lipid radicals. The HCT-116 parent cell line showed evidence of robust ferroptosis, and the deletion of p53 in this cell line almost completely protected the cells from this form of cell death (Figure 5). In contrast, the SW48 parent cell line possessed only modest activity of ferroptosis, and more importantly the G12D mutation in KRAS did not have any effect on this process (Figure 5). These differential effects of p53 loss and KRAS mutation on ferroptosis occurred despite the fact that both induced SLC7A11 expression and function. This suggests that p53 loss is the predominant factor in the protection of colon cancer cells from ferroptosis with little/no participation by the oncogenic mutation in KRAS in the process.

Preprints.org (www.preprints.org) | NOT PEER-REVIEWED | Posted: 4 April 2024 doi:10.20944/preprints202404.0092.v2

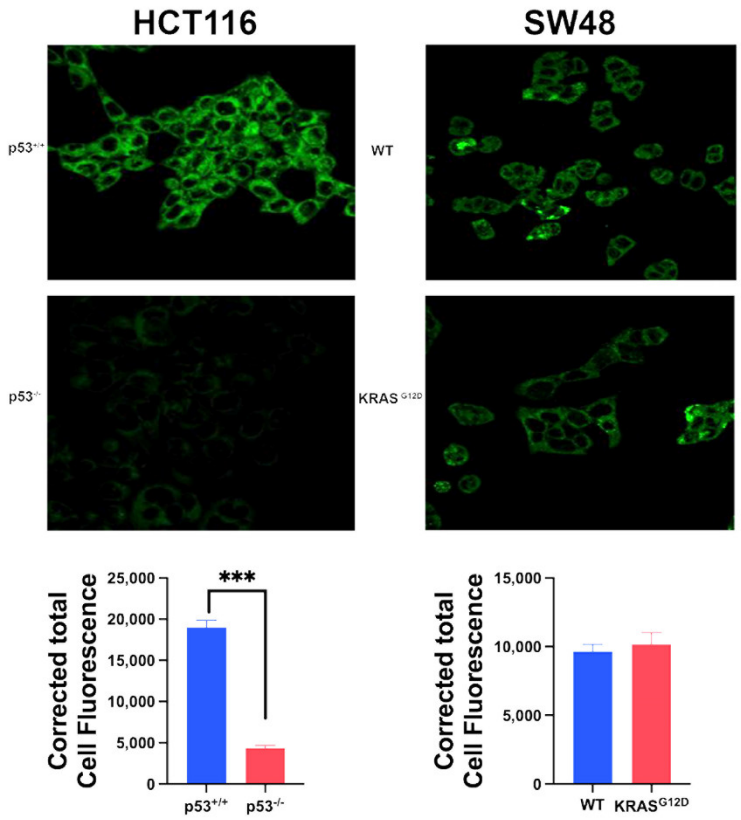

Figure 5. Basal ferroptosis activity in the two pairs of isogenic colon cancer cells with and without p53 (HCT-116) and with and without G12D mutation in KRAS (SW48) as assessed by fluorescence detection of lipid radicals. Quantification of the fluorescence signals are also given (mean ± S.E. for three independent experiments). ***, $p < 0.001$. When not specified, the difference is not significant.

3.7. Influence of p53 Loss and KRAS-G12D Mutation on Various Factors that are Relevant to Ferroptosis

Ferroptosis is a non-apoptotic, non-necroptotic, and caspase-independent cell death caused excessive oxidation of double bonds in polyunsaturated fatty acids in membrane-associated phospholipids. This involves reactive oxygen species (ROS) such as H_2O_2 and the process generates lipid peroxide radicals and malondialdehyde (MDA). The culprit in the whole process is excessive labile iron in Fe^{2+} form that converts H_2O_2 into hydroxyl radical which initiates oxidation of the membrane lipids. Glutathione protects against ferroptosis because of its ability to remove H_2O_2 and lipid peroxides. To assess the role of these factors in ferroptosis in the two pairs of isogenic colon cancer cell lines in the present study, we quantified most of these parameters. The iron assay employed in our study measures only Fe^{2+}, which is involved in the Fenton reaction. Loss of p53 in HCT-116 cells increased the cellular levels of Fe^{2+} whereas the presence of the oncogenic mutation G12D in SW48 cells decreased the levels (Figure 6). ROS levels were lower in SW48 cells than in HCT-116 cells, but neither the loss of p53 nor the presence of G12D mutation in KRAS had any significant effect on ROS levels in the respective cell lines (Figure 7). Even though the levels of glutathione (GSH) remained the same in control and p53-null HCT-116 cells, MDA levels, an indicator of ferroptosis, was lower in *p53*-null cells (Figure 7). In contrast, GSH levels and MDA levels were both increased in SW48 cells harboring G12D mutation in KRAS compared to the parent SW48 cells (Figure 7). Obviously, these parameters do not directly correlate with the ferroptosis status of the four cell lines, most likely because of the intricate back-and-forth relationship between oxidative stress and GSH where oxidative stress induces GSH synthesis and increase in GSH levels suppress oxidative stress. The same is true with Fe^{2+} and p53 because increased iron/heme promotes degradation of p53 whereas loss of p53 increases iron levels. However, the ferroptosis status is the final outcome that is important to understand the role of p53 loss and oncogenic mutations in KRAS in cancer cells.

 doi:10.20944/preprints202404.0092.v2

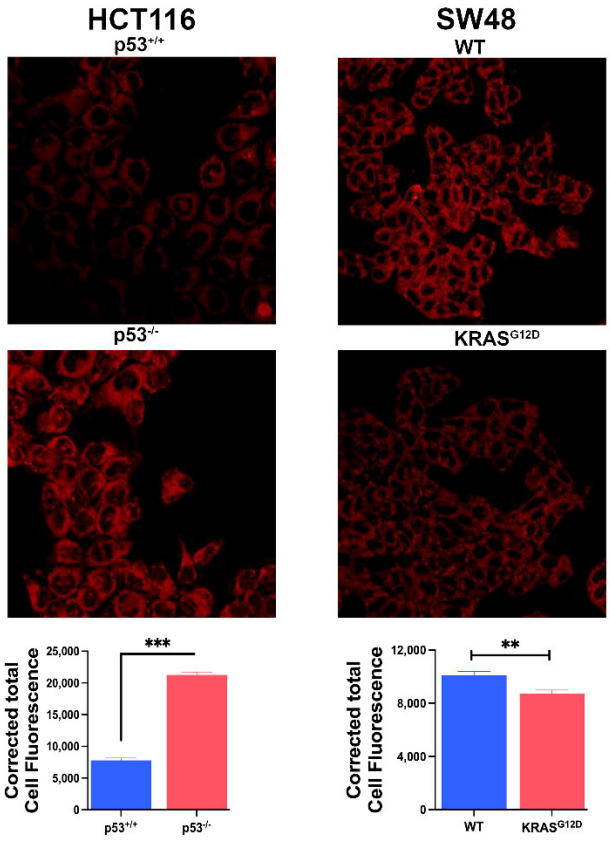

Figure 6. Iron levels in the two isogenic cell lines with and without p53 (HCT-116) and with and without G12D mutation in KRAS (SW48). The fluorescence signals were also quantified (data given as mean ± S.E.). **, $p < 0.01$; ***, $p < 0.001$.

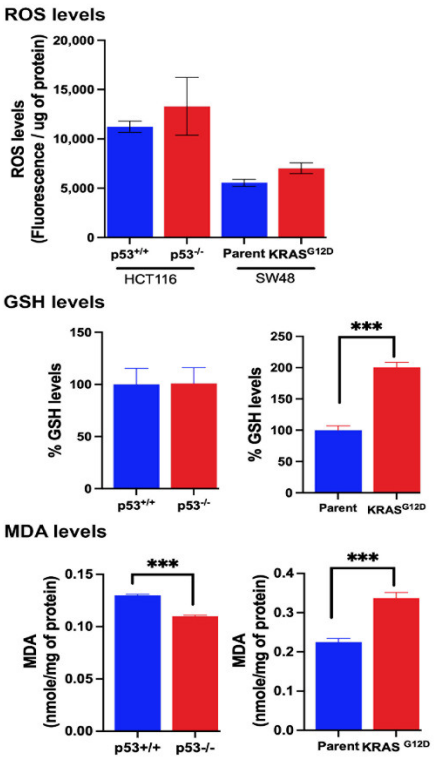

 doi:10.20944/preprints202404.0092.v2

Figure 7. Basal levels of ROS, GSH and MDA. Data (mean ± S.E.) are from three independent experiments. ***, $p < 0.001$. When not specified, the differences were not statistically significant.

3.8. Effects of Niclosamide on Intracellular pH and the Transport Function of SLC38A5 and SLC7A11

Niclosamide is known to have multiple effects in cancer cells, influencing several signaling pathways [55–57]. Nonetheless, we focused in the present study on the effects of this drug on intracellular pH and on the transport activities of SLC38A5 and SLC7A11 because of their direct connection to macropinocytosis (intracellular pH and SLC38A5) and ferroptosis (SLC7A11). Our recent studies with breast cancer cell lines have demonstrated that niclosamide causes intracellular acidification and also inhibits SLC38A5, both leading to suppression of macropinocytosis [29]. Niclosamide is also a potent inhibitor of SLC7A11 in breast cancer cell lines, consequently leading to induction of ferroptosis [30]. The effect on intracellular pH is related to the function of niclosamide as a protonophore (i.e., a H^+ channel) [58,59] whereas the inhibitory effect of the drug on SLC38A5 and SLC7A11 is the result of its direct interaction with the two transporters. In the present study, we tested if niclosamide had similar effects in colon cancer cell lines. In all four cell lines we examined in the present study, niclosamide (2.5 μM) caused a decrease in intracellular pH, leading to cellular acidification (Figure 8). The rate of acidification varied among the four cell lines; it was the highest in HCT-116 cells with wild type p53 and the lowest in SW48 cells with the oncogenic mutation G12D in KRAS. Another thing noticeable was the influence of p53 loss in HCT-116 cells and KRAS-G12D mutation in SW48 cells. Both these changes are oncogenic, and these changes significantly decreased the rate of acidification by niclosamide. This suggests that genetic changes related to p53 and KRAS that promote cancer are associated with significant impact on the control of intracellular pH by effectively protecting the cells from acidification.

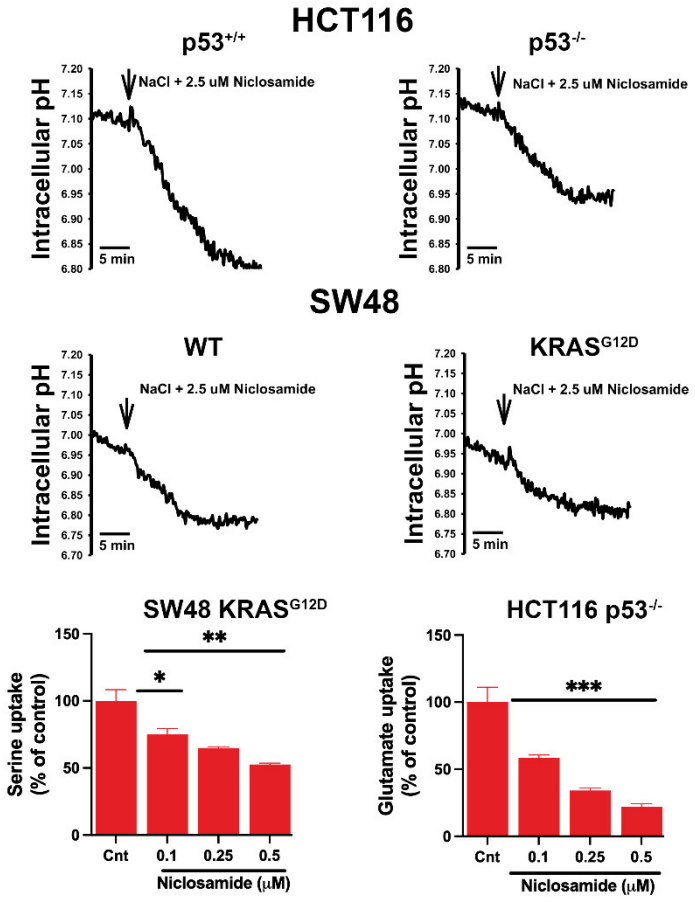

Preprints.org (www.preprints.org) | NOT PEER-REVIEWED | Posted: 4 April 2024 doi:10.20944/preprints202404.0092.v2

Figure 8. Effects of niclosamide on intracellular pH in all four cell lines and on the transport activity of SLC38A5 in SW48 cells with G12D mutation in KRAS and on the transport activity of SLC7A11 in p53-null HCT-116 cells. Data are given as mean ± S.E. *, $p < 0.05$; **, $p < 0.01$; ***, $p < 0.001$.

We also monitored the effect of niclosamide on the transport activities of SLC38A5 (Li^+-coupled serine uptake in SW48 cells with KRAS-G12D) and SLC7A11 (Na^+-independent glutamate uptake in *p53*-null HCT-116 cells) (Figure 8). There was no specific reason to select these two cell lines except that p53 loss and KRAS-G12D mutation represented oncogenic changes that are relevant to promotion of cancer growth and that these cell lines showed greatest activity for the respective transporters. We found that niclosamide had robust inhibitory effect on the transport functions of SLC38A5 as well as SLC7A11. Even at concentrations less than 0.5 μM, the inhibition on both transporters was 50% or greater.

3.9. Inhibition of Macropinocytosis by Niclosamide

Based on our previous studies with breast cancer cells [29,30], the ability of niclosamide to induce intracellular acidification and inhibit SLC38A5 is expected to suppress macropinocytosis. We tested this by monitoring macropinocytosis-mediated cellular entry of TMR-dextran in all four colon cancer cell lines with a 30-min preincubation with and without niclosamide (5 μM). Irrespective of the presence or absence of oncogenic changes in p53 and KRAS, niclosamide showed a dramatic suppressive effect on macropinocytosis (Figure 9). The inhibition was 70% or greater in all four cell lines.

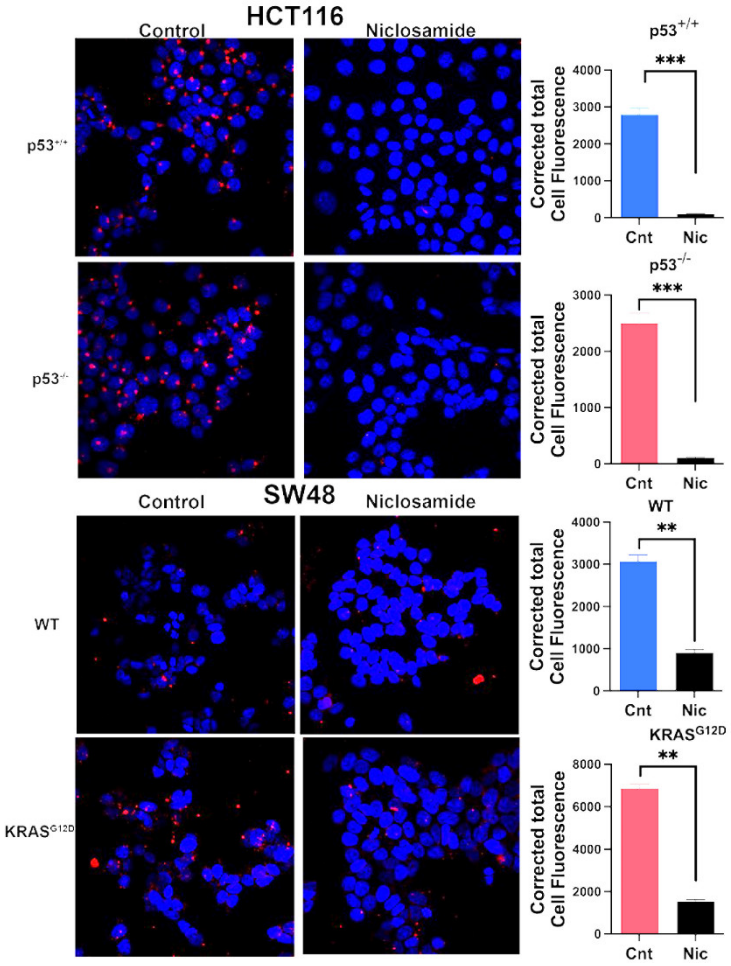

Figure 9. Effects of niclosamide (5 μM) on macropinocytosis in the two pairs of isogenic cell lines. Immunofluorescence images as well as quantification of the fluorescence signals are given. Data are given as mean ± S.E. **, $p < 0.01$; ***, $p < 0.001$.

 doi:10.20944/preprints202404.0092.v2

3.10. Induction of Ferroptosis by Niclosamide

The marked inhibitory effect of niclosamide on the transport activity of SLC7A11 is expected to promote ferroptosis. We tested this by monitoring cellular levels of lipid radicals with a fluorescent probe following a 30-min preincubation with and without niclosamide (5 μM). The data from isogenic HCT-116 cells with and without p53 are given in Figure 10. The parent cell line which harbors wild type p53, ferroptosis was robust even under basal conditions without exposure to niclosamide, and niclosamide did not have any effect on ferroptosis in this cell line. In contrast, ferroptosis was almost undetectable in HCT-116 cells in which p53 was deleted. This was seen in the earlier experiment described in Figure 5. But, in this cell line, niclosamide was able to induce ferroptosis to a marked extent in a dose-dependent manner. A significant induction of ferroptosis was noticeable even at 0.25 μM niclosamide and the maximal effect was seen with less than 5 μM niclosamide. In SW48 cells, there was a modest activity of ferroptosis under basal conditions without exposure to niclosamide, which was not affected by the presence or absence of G12D mutation in KRAS as seen in an earlier experiment (Figure 5). However, exposure to niclosamide markedly induced ferroptosis in this cell line irrespective of the presence or absence of the oncogenic mutation G12D in KRAS, and the effect was dose-dependent (Figure 11). The potentiating effect of niclosamide on ferroptosis was noticeable even at 0.25 μM and the maximal effect was observed at niclosamide concentrations less than 5 μM. With *p53*-null HCT-116 cells, we confirmed that the process induced by niclosamide in increasing the fluorescent signals for lipid radicals was indeed ferroptosis by demonstrating the blockade of the process by ferrostatin (Figure 12), a radical-trapping antioxidant and a selective blocker of ferroptosis [60,61].

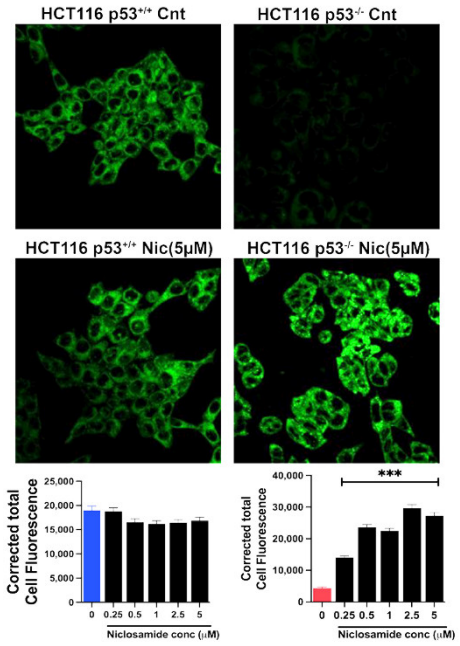

Figure 10. Induction of ferroptosis by niclosamide (5 μM) in HCT116 cells with and without p53. Quantification of the fluorescence signals (mean ± S.E.) are also given. ***, $p < 0.001$. When not specified, the differences were not statistically significant.

Preprints.org (www.preprints.org) | NOT PEER-REVIEWED | Posted: 4 April 2024 doi:10.20944/preprints202404.0092.v2

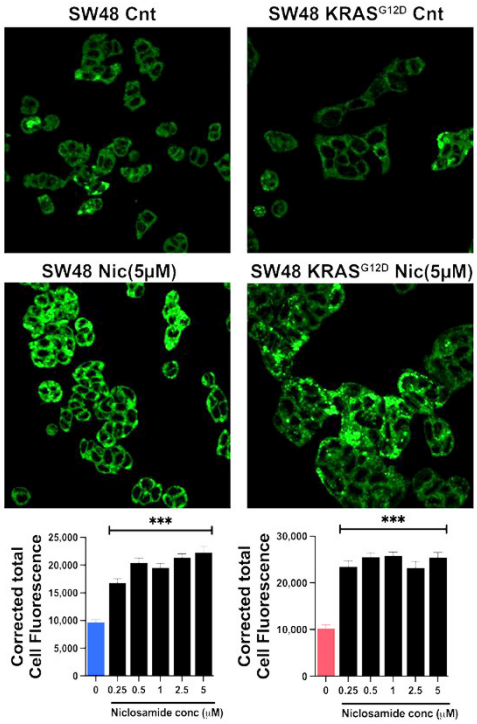

Figure 11. Induction of ferroptosis by niclosamide (5 μM) in SW48 cells with and without G12D mutation in KRAS. Quantification of the fluorescence signals (mean ± S.E.) are given. ***, $p < 0.001$.

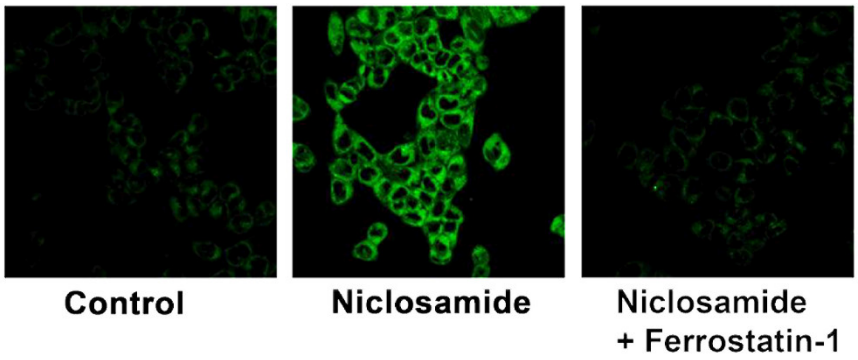

Figure 12. Blockade of niclosamide (5 μM)-induced ferroptosis by ferrostatin (10 μM) in *p53*-null HCT116 cells.

3.11. Effects of Niclosamide on Cellular Levels of ROS, GSH and MDA

Since we observed profound ability of niclosamide to induce ferroptosis in colon cancer cells, we monitored the influence of this drug on cellular levels of reactive oxygen species (ROS), glutathione (GSH), and malondialdehyde (MDA), all of which are directly related to the process of ferroptosis. Cells were treated with 2.5 μM niclosamide for 24 h and then the cells were lysed and used for measurements of ROS, GSH, and MDA. The results showed that niclosamide increased ROS levels and decreased GSH levels, which was accompanied with an increase in MDA levels; these findings were consistent in all four colon cancer cell lines (HCT-116 cells with and without p53, SW48 cells with and without G12D mutation in KRAS) (Figure 13).

Preprints.org (www.preprints.org) | NOT PEER-REVIEWED | Posted: 4 April 2024 doi:10.20944/preprints202404.0092.v2

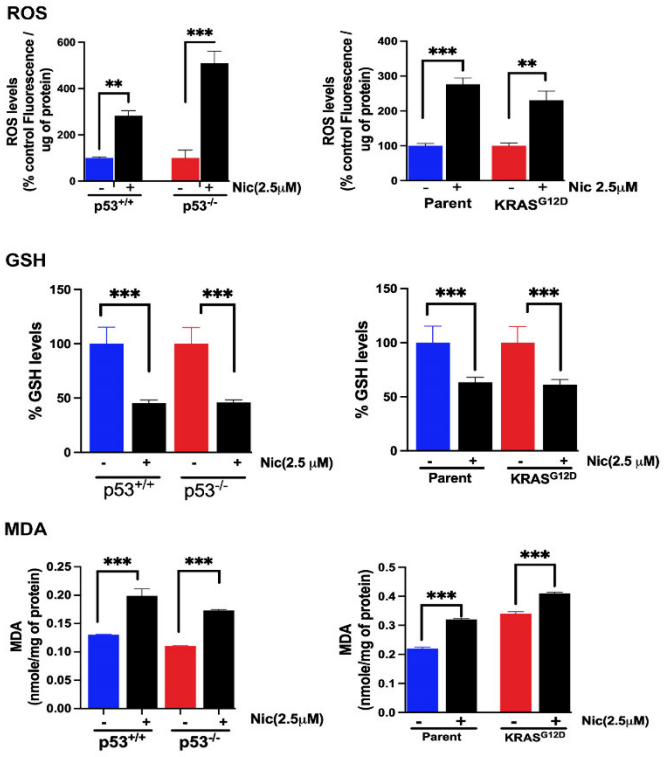

Figure 13. Effects of niclosamide on cellular levels of ROS, GSH, and MDA. The cells were treated with niclosamide (2.5 μM) for 24 h. Data are given as mean ± S.E. **, $p < 0.01$; ***, $p < 0.001$.

3.12. Effects of Niclosamide on Cellular Levels of Ferritin Heavy Chain and Glutathione Peroxidase

We also monitored the impact of niclosamide treatment (2.5 μM; 24 h treatment) on the protein levels for the ferritin heavy chain FTH1 as well as for the antioxidant enzyme glutathione peroxidase (GPX). Niclosamide decreases the levels of FTH1 in HCT-116 and SW48 cells independent of the presence or absence of p53 or KRAS-G12D mutation (Figure 14). For GPX, the decrease was evident only SW48 cells with and without the KRAS-G12D mutation and in *p53*-null HCT-116 cells.

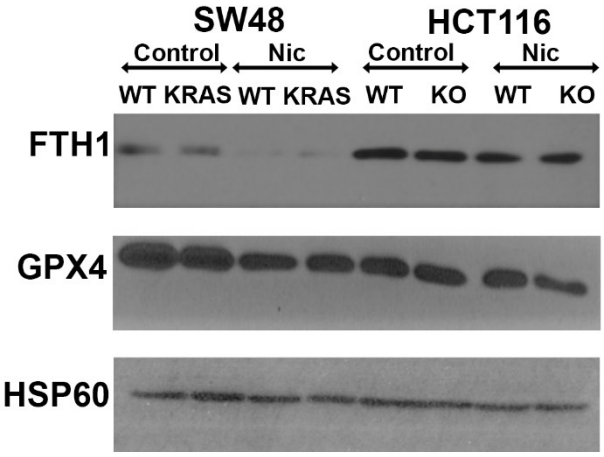

Figure 14. Effects of niclosamide treatment (2.5 μM; 24 h) on FTH1 and GPX protein levels.

3.13. Effects of Niclosamide on Cell Viability/Proliferation and Colony Formation

The experiments detailed in the previous sections of this study have shown that niclosamide suppresses macropinocytosis, an effective nutrient-acquiring mechanism, and at the same induces

 doi:10.20944/preprints202404.0092.v2

ferroptosis, an iron-dependent cell death process. Therefore, these effects are expected to have a significant detrimental effect on cell viability, cell proliferation, and colony-formation ability of colon cancer cells. We addressed this issue by examining the influence of niclosamide on these processes in all four cell lines. Niclosamide markedly inhibited cell viability and cell proliferation in a dose-dependent and exposure time-dependent manner as monitored by MTT assay (Figure 15). Even at niclosamide concentrations as low as 2 μM, the inhibitory effect on cell viability and proliferation was 50% or greater. With a 72-h treatment, the inhibition reached >75%. Interestingly, the inhibition appeared to be more potent in cells with oncogenic changes in p53 and KRAS. The effects were similar when the colony-forming ability of these cells was examined (Figure 16). The inhibition was significant even at concentrations of niclosamide as low as 0.5 μM; in three out of the four cell lines, the inhibition was 75% or greater at 1 μM niclosamide.

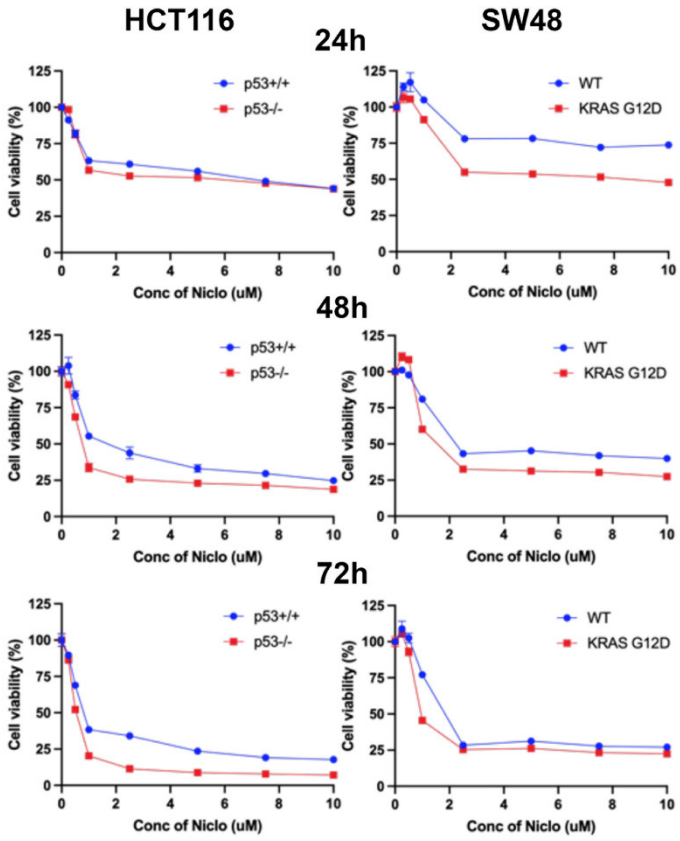

Figure 15. Inhibition of cell viability and proliferation by niclosamide as monitored by MTT assay in all four cell lines (HCT-116 cells with and without p53; SW48 cells with and without KRAS-G12D mutation). Cell viability was calculated as percent of control cells without treatment with niclosamide. Data (mean ± S.E.) are from three independent experiments.

 doi:10.20944/preprints202404.0092.v2

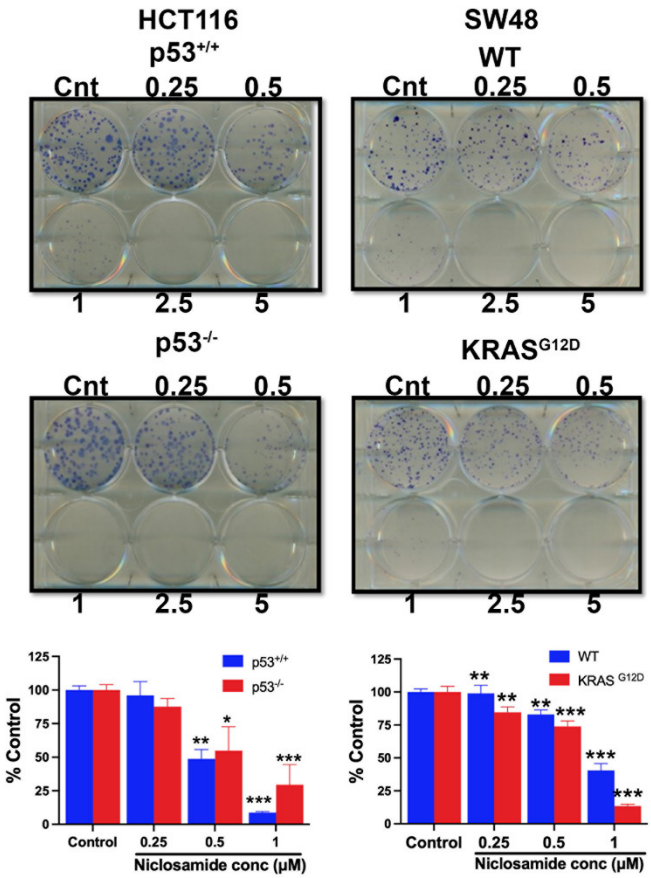

Figure 16. Effects of niclosamide on colony-forming ability in HCT-116 cells with and without p53 and in SW48 cells with and without KRAS-G12D mutation. Data (mean ± S.E.) are for three independent experiments. *, $p < 0.05$; **, $p < 0.01$; ***, $p < 0.001$. When not specified, the differences were not statistically significant.

4. Discussion

Recently, we published reports on macropinocytosis and ferroptosis in triple-negative breast cancer cell lines MB231 and TXBR-100 and on the effects of the anti-helminthic drug niclosamide on these two processes [29,30,43]. In these cell lines, niclosamide caused intracellular acidification and had opposing effects on macropinocytosis (suppression) and ferroptosis (induction). However, we did not examine the influence of p53 and KRAS on macropinocytosis and ferroptosis in these cell lines. Even though mutant p53 is common in breast cancer, mutations in KRAS are not frequent (<5%). Among the breast cancer cell lines, only MB231 possesses mutant p53 and also mutant KRAS (G13D) [62–64]. The mutational status of p53 and KRAS is not known for TXBR-100, a patient-derived breast cancer cell line we used in these previous studies. As such, the previously published studies did not focus on the differential influence of p53 and KRAS mutations on macropinocytosis and ferroptosis in breast cancer cells. We also did not know if the actions of niclosamide as a suppressor of macropinocytosis and an inducer of ferroptosis that we observed in breast cancer cells are dependent on the mutational status of p53 and/or KRAS. The present study represents the first on this topic, but done with colon cancer cells where isogenic cell lines are available with and without p53 and KRAS mutation. Moreover, such studies are more relevant to colon cancer where KRAS mutations are much more prevalent than in breast cancer cells (30-50% versus <5%).

Glutamine is a critical amino acid for cancer cell growth and proliferation based on its connection to mTOR activation, nucleotide and protein synthesis, ATP production, lipid synthesis, and antioxidant machinery [65]. Among the various glutamine transporters in mammalian cells [20], SLC38A5 is unique because its transport function is associated with intracellular alkalinization [66]

 doi:10.20944/preprints202404.0092.v2

and one-carbon metabolism [67]. This transporter has come to prominence in recent years because of the recognition that it is upregulated in breast cancer [43,68] and pancreatic cancer [69,70] and is coupled to chemoresistance [68,70,71]. The role of SLC38A5 in colon cancer has not yet been investigated even though it is expressed in the intestinal tract [66].

The finding that SLC38A5 is involved in macropinocytosis is a recent observation [43]. We hypothesized this involvement primarily based on the functional feature of the transporter as an amino-acid-dependent Na^+/H^+ exchanger and the known fact that Na^+/H^+ exchanger is an inducer of macropinocytosis. The role of Na^+/H^+ exchanger in macropinocytosis is also the basis for the widespread use of ethylisopropylamiloride and dimethylamiloride, potent inhibitors of the exchanger, as specific blockers of macropinocytosis [72].

The salient findings in the present study with regard to macropinocytosis in colon cancer cells can be summarized as follows: (i) The oncogenic mutation G12D in KRAS is the driver of macropinocytosis with apparently no involvement of p53; (ii) The oncogenic changes in p53 (loss of function) and KRAS (activating mutation) elicit opposite effects on SLC38A5 expression, and the induction of the transporter by KRAS-G12D mutation is at least partly responsible for the increased activity of macropinocytosis seen in SW48 cells with the mutation; (iii) The increase in SLC38A5 expression elicited by KRAS-G12D mutation is mediated by the transcriptional activity of the oncogene Myc; (iv) SLC38A5 is also a target for p53, but this transcription factor functions as an inducer of SLC38A5 expression in contrast to its action as a suppressor of SLC7A11 expression; (v) Niclosamide is a potent suppressor of macropinocytosis in colon cancer cells irrespective of whether or not the cells harbor oncogenic changes in p53 and KRAS; (vi) The ability of niclosamide to cause intracellular acidification and to inhibit SLC38A5 is at least partly responsible for this effect.

Ferroptosis is being increasingly recognized as one of the most important vulnerabilities and an Achilles' heel in cancer cells because these cells have to navigate between their obligate need to accumulate iron to support their growth and proliferation and at the same time the challenge to protect themselves from iron-induced cell death [13,14,73,74]. The tumor suppressor p53 and the amino acid transporter SLC7A11 are at the center of these two opposing phenomena. When cancer cells accumulate iron, heme levels increase. p53 is a heme-binding protein, and when heme binds to p53, the complex gets degraded in proteasomes [23]. As a consequence, excess iron in cancer cells leads to p53 depletion. SLC7A11 is the most important protector of cancer cells from iron-induced ferroptosis because of its ability to increase cellular levels of glutathione. The expression of this transporter is suppressed by p53 [23]. As such, p53 loss induced by excess iron/heme results in increased expression of SLC7A11 in cancer cells, thus protecting the cells from ferroptosis. This phenomenon also occurs in hemochromatosis, a genetic disorder associated with iron overload, where iron accumulation leads to increased heme and consequent p53 loss and also increased susceptibility to colon cancer [75]. The present study provides confirmation to the functional interaction among p53, SLC7A11, and ferroptosis. Deletion of p53 in HCT-116 cells potentiates the expression and function SLC7A11 and as a result ferroptosis becomes almost undetectable in these cells. Another important finding from the present study is that it is p53, not KRAS, that plays the key role in the control of ferroptosis. However, we found that the oncogenic mutation G12D in KRAS does induce the expression of SLC7A11 in SW48 cells even in the presence of p53. These findings suggest that KRAS activation in cancer cells has potential to provide protection against ferroptosis under conditions where p53 is still functional. It is interesting to note the similarity in the transcriptional activation of SLC7A11 between the oncogenic changes in p53 (loss of function) and KRAS (activating mutation), both leading to induction of SLC7A11 expression. This is in contrast to their effects on SLC38A5 expression where they play opposing roles.

In addition to providing important new information on the opposing roles of oncogenic changes in p53 and KRAS in colon cancer cells not only in terms of macropinocytosis and ferroptosis but also in terms of the control of SLC38A5 and SLC7A11 expression, the present study highlights the therapeutic potential of the FDA-approved anti-helminthic drug niclosamide. The findings that the drug elicits opposing effects on macropinocytosis and ferroptosis in colon cancer cells irrespective of the presence or absence of oncogenic changes in p53 and KRAS are the salient features of the present

 doi:10.20944/preprints202404.0092.v2

study. The drug blocks macropinocytosis, thus interfering with an important route of nutrient acquisition in cancer cells; at the same time, it also induces ferroptosis, a key vulnerability in cancer cells. These effects are at least partly due to the ability of the drug to inhibit the transport function of SLC38A5 (relevant to macropinocytosis) and SLC7A11 (relevant to ferroptosis). It is also important to point out here that the potency of niclosamide as an inhibitor of SLC7A11 (IC_{50}, <0.25 μM) is greater than most of the inhibitors, including erastin, reported thus far in the literature [76]. We found a similar IC_{50} value in triple-negative breast cancer cells [30]. Even though derivatives of erastin have been developed recently with much greater potency to inhibit SLC7A11 (IC_{50} values in the low-nanomolar range) [77], niclosamide may have an advantage in terms of therapeutic use for cancer therapy because of its feature as an already FDA-approved drug that has been in use in humans for several decades. The often pointed out disadvantage of niclosamide as an anticancer agent is its poor oral bioavailability [78,79]. This may be a valid argument for the use of the drug to treat cancers of non-colonic origin but not for its use to treat colon cancer. Niclosamide is active in the lumen of the intestinal tract when given for the treatment of helminth infections; therefore, the drug will have access to cancer cells in the colon to elicit its anticancer effects. With this rationale, we conclude that the results of the present study underscore the therapeutic potential of niclosamide in the treatment of colorectal cancer. Even for other cancers of non-colonic origin, there could be effective strategies such as nano-formulations or chemical modifications to improve the oral bioavailability of niclosamide to harness its efficacy as an anticancer drug.

5. Conclusions

There are two important conclusions that can be gleaned from the present study: (i) Macropinocytosis is a pro-growth process in cancer which is primarily promoted by activating mutations in KRAS in colon cancer cells whereas ferroptosis is an anti-growth process in cancer which is primarily blocked by loss of p53 in colon cancer cells; (ii) the anti-helminthic niclosamide is a potent blocker of macropinocytosis and a potent inducer of ferroptosis in colon cancer cells, both effects having a marked anticancer impact, irrespective of the presence or absence of oncogenic changes in p53 and KRAS.

Supplementary Materials: The following supporting information can be downloaded at: www.mdpi.com/xxx/s1, Table S1: Primer sequences for RT-PCR; Figures: Original western blots.

Author Contributions: Conceptualization, N.T.N., S.S. and V.G; methodology, N.T.N., S.R.S., G.D.N., and S.S.; validation, S.S. and V.G.; investigation, N.T.N., S.R.S., G.D.N., and S.S.; writing—original draft preparation, V.G.; writing—review and editing, N.T.N., S.S. and Y.D.B.; supervision, S.S. and V.G.; project administration, V.G. All authors have read and agreed to the published version of the manuscript.

Funding: This research received no external funding.

Institutional Review Board Statement: Not applicable.

Data Availability Statement: The authors confirm that the data supporting the findings of this study are given in their entirety within this manuscript and its supplementary material.

Conflicts of Interest: The authors declare no conflicts of interest.

References

1. Siegel, R.L.; Wagle, N.S.; Cercek, A.; Smith, R.A.; Jemal, A. Colorectal cancer statistics, 2023. *CA Cancer J. Clin*. **2023**, *73*, 233-254.
2. https://seer.cancer.gov/statfacts/html/colorect.html
3. https://www.who.int/news-room/fact-sheets/detail/colorectal-cancer
4. Araghi, M.; Soerjomataram, I.; Jenkins, M.; Brierley, J.; Morris, E.; Bray, F.; Arnold, M. Global trends in colorectal cancer mortality: projections to the year 2035. *Int. J. Cancer* **2019**, *144*, 2992-3000.
5. Valle, L. Genetic predisposition to colorectal cancer: Where we stand and future perspectives. *World J. Gastroenterol*. **2014**, *20*, 9828-9849.
6. Strate, L.L.; Syngal, S. Hereditary colorectal cancer syndromes. *Cancer Causes Control* **2005**, *16*, 201-213.

7. Hryhorowicz, S.; Kaczmarek-Rys, M.; Lis-Tanas, E.; Porowski, J.; Szuman, M.; Grot, N.; Kryszczynska, A.; Paszkowski, J.; Banasiewicz, T.; Plawski, A. Strong hereditary predispositions to colorectal cancer. *Genes (Basel)* **2022**, *13*, 2326.
8. Zhong, Z.A.; Michalski, M.N.; Stevens, P.D.; Sall, E.A.; Williams, B.O. Regulation of Wnt receptor activity: Implications for therapeutic development in colon cancer. *J. Biol. Chem*. **2021**, *296*, 100782.
9. Boutin, A.T.; Liao, W.T.; Wang, M.; Hwang, S.S.; Karpinets, T.V.; Cheung, H.; Chu, G.C.; Jiang, S.; Hu, J.; Chang, K.; et al. Oncogenic Kras drives invasion and maintains metastases in colorectal cancer. *Genes Dev*. **2017**, *31*, 370-382.
10. Nakayama, M.; Oshima, M. Mutant P53 in colon cancer. *J. Mol. Cell. Biol*. **2019**, *11*, 267-276.
11. Encarnacion-Rosado, J.; Kimmelman, A.C. Harnessing metabolic dependencies in pancreatic cancers. *Nat. Rev. Gastroenterol. Hepatol.* **2021**, *18*, 482-492.
12. Recouvreux, M.V.; Commisso, C. Macropinocytosis: A metabolic adaptation to nutrient stress in cancer. *Front. Endocrinol. (Lausanne)*, **2017**, *8*, 261.
13. Stockwell, B.R. Ferroptosis turns 10: Emerging mechanisms, physiological functions, and therapeutic applications. *Cell* **2022**, *185*, 2401-2421.
14. Dixon, S.J.; Stockwell, B.R. The role of iron and reactive oxygen species in cell death. *Nat. Chem. Biol*. **2014**, *10*, 9-17.
15. Timar, J.; Kashofer, K. Molecular epidemiology and diagnostics of KRAS mutations in human cancer. *Cancer Metastasis Rev*. **2020**, *39*, 1029-1038.
16. Nagy, J.A.; Dvorak, A.M.; Dvorak, H.F. Vascular permeability, angiogenesis, and stroma generation. *Cold Spring Harb. Perspect. Med*. **2012**, *2*, a006544.
17. Nagl, L.; Horvath, L.; Pircher, A.; Wolf, D. Tumor endothelial cells (TECs) as potential immune directors of the tumor microenvironment – New findings and future perspectives. *Front. Cell Dev. Biol*. **2020**, *8*, 766.
18. Broer, S. Amino acid transporters as targets for cancer therapy: Why, where, when, and how. *Int. J. Mol. Sci*. **2020**, *21*, 6156.
19. Bhutia, Y.D.; Babu, E.; Ramachandran, S.; Ganapathy, V. Amino acid transporters in cancer and their relevance to "glutamine addiction": Novel targets for the design of a new class of anticancer drugs. *Cancer Res.* **2015**, *75*, 1782–1788.
20. Bhutia, Y.D.; Ganapathy, V. Glutamine transporters in mammalian cells and their functions in physiology and cancer. *Biochim. Biophys. Acta* **2016**, *1863*, 2531–2539.
21. Torti, S.V.; Torti, F.M. Iron: The cancer connection. *Mol. Aspects Med*. **2020**, *75*, 100860.
22. Sainkow, K. Role of iron in cancer. *Semin. Cancer Biol*. **2021**, *76*, 189-194.
23. Shen, J.; Sheng, X.; Chang, Z.; Wu, Q.; Wang, S.; Xuan, Z.; Li, D.; Wu, Y.; Kong, X.; Yu, L.; et al. Iron metabolism regulates p53 signaling through direct heme-p53 interaction and modulation of p53 localization, stability, and function. *Cell Rep*. **2014,** *7*, 180-193.
24. Bhutia, Y.D.; Ogura, J.; Grippo, P.J.; Torres, C.; Sato, T.; Wachtel, M.S.; Ramachandran, S.; Babu, E.; Sivaprakasam, S.; Rajasekaran, D.; et al. Chronic exposure to excess iron promotes EMT and cancer via p53 loss in pancreatic cancer. *Asian J. Pharm. Sci.* **2020**, *15*, 237-251.
25. https://www.cancer.org/cancer/types/colon-rectal-cancer/treating.html
26. https://www.cancer.gov/types/colorectal/patient/colon-treatment-pdq
27. Chen, W.; Mook, R.A.; Premont, R.T.; Wang, J. Niclosamide: Beyond an antihelminthic drug. *Cell Signal*. **2018**, *41*, 89-96.
28. Andrews, P.; Thyssen, J.; Lorke, D. The biology and toxicology of molluscicides, Bayluscide. *Pharamcol. Ther*. **1982**, *19*, 245-295.
29. Sennoune, S.R.; Dharmalingam-Nandagopa, G.; Ramachandran, S.; Mathew, M.; Sivaprakasam, S.; Jaramillo-Martinez, V.; Bhutia, Y.D.; Ganapathy, V. Potent inhibition of macropinocytosis by niclosamide in cancer cells: A novel mechanism for the anticancer efficacy for the anti-helminthic. *Cancers* **2023,** *15*, 759.
30. Mathew, M.; Sivaprakasam, S.; Dharmalingam-Nandagopal, G.; Sennoune, S.R.; Nguyen, N.T.; Jaramillo-Martinez, V.; Bhutia, Y.D.; Ganapathy, V. Induction of oxidative stress and ferroptosis in triple-negative breast cancer cells by niclosamide via blockade of the function and expression of SLC38A5 and SLC7A11. *Antioxidants* **2024**, *13*, 291.
31. Fennell, M.; Commisso, C.; Ramirez, C.; Garippa, R.; Bar-Sagi, D. High-content, full genome siRNA screen for regulators of oncogenic HRAS-driven macropinocytosis. *Assay Drug Dev. Technol*. **2015**, *13*, 347-355.

 doi:10.20944/preprints202404.0092.v2

32. Commisso, C.; Flinn, R.J.; Bar-Sagi, D. Determining the macropinocytic index of cells through a quantitative image-based assay. *Nat. Protoc*. **2014**, *9*, 182-192.
33. Matsuoka, Y.; Yamada, K.I. Detection and structural analysis of lipid-derived radicals in vitro and in vivo. *Free Radic. Res*. **2021**, *55*, 441-449.
34. Yamada, K.I.; Mito, F.; Matsuoka, Y.; Ide, S.; Shikimachi, K.; Fujiki, A.; Kusakabe, D.; Ishida, Y.; Enoki, M.; Tada, A.; et al. Fluorescence probes to detect lipid-derived radicals. *Nat. Chem. Biol*. **2016**, *12*, 608-613.
35. Kim, H.; Xue, X. Detection of total reactive oxygen species in adherent cells by 2′.7′-dichlorodihydrofluorescein diacetate staining. *J. Vis. Exp*. **2020**, *160*, 10.3791/60682.
36. Yang, J.; Zhang, W.; Evans, P.W.; Chen, X.; He, X.; Liu, C. Adenomatous polyposis coli (APC) differentially regulates β-catenin phosphorylation and ubiquitination in colon cancer cells. *J. Biol. Chem*. **2006**, *281*, 17751-17757.
37. Ahmed, D.; Eide, P.W.; Ellertsen, I.A.; Danielsen, S.A.; Eknaes, M.; Hektoen, M.; Lind, G.E.; Lothe, R.A. Epigenetic and genetic features of 24 colon cancer cell lines. *Oncogenesis* **2013**, *2*, e71.
38. Berg, K.C.G.; Eide, P.W.; Ellertsen, I.A.; Johannessen, B.; Bruun, J.; Danielsen, S.A.; Bjornslett, M.; Meza-Zepeda, L.A.; Eknaes, M.; Lind, G.E.; et al. Multi-omics of 34 colorectal cancer cell lines – a resource for biomedical studies. *Mol. Cancer* **2017**, *16*, 116.
39. Proto, M.C.; Fiore, D.; Piscopo, C.; Francesschelli, S.; Bizzarro, V.; Laezza, C.; Lauro, G.; Feoli, A.; Tosco, A.; Bifulco, G.; et al. Inhibition of Wnt/β-catenin pathway and histone acetyltransferase activity by Rimonabant: a therapeutic target for colon cancer. *Sci. Rep*. **2017**, *7*, 11678.
40. Medico, E.; Russo, M.; Picco, G.; Cancelliere, C.; Valtorta, E.; Corti, G.; Buscarino, M.; Isella, C.; Lamba, S.; Martinoglio, B.; et al. The molecular landscape of colorectal cancer cell lines unveils clinically actionable kinase targets. *Nat. Commun*. **2015**, *6*, 7002.
41. Veettil, M.V.; Kumar, B.; Ansari, M.A.; Dutta, D.; Iqbal, J.; Gjyshi, O.; Bottero, V.; Chandran, B. ESCRT-o component Hrs promotes macropinocytosis of Kaposi's sarcoma-associated Herpesvirus in human dermal microvascular endothelial cells. *J. Virol*. **2016**, *90*, 3860-3872.
42. Lin, H.P.; Singla, B.; Ahn, W.; Ghoshal, P.; Blahove, M.; Cherian-Shaw, M.; Chen, A.; Haller, A.; Hui, D.Y.; Dong, K.; et al. Receptor-independent fluid-phase micropinocytosis promotes arterial foam cell formation and atherosclerosis. *Sci. Transl. Med*. **2022**, *14*, eadd2376.
43. Ramachandran, S.; Sennoune, S.R.; Sharma, M.; Thangaraju, M.; Suresh, V.V.; Sneigowski, T.; Bhutia, Y.D.; Pruitt, K.; Ganapathy, V. Expression and function of SLC38A5, an amino acid-coupled Na^+/H^+ exchanger, in triple-negative breast cancer and its relevance to macropinocytosis. *Biochem. J*. **2021**, *478*, 3957-3976.
44. Bhutia, Y.D.; Mathew, M.; Sivaprakasam, S.; Ramachandran, S.; Ganapathy, V. Unconventional functions of amino acid transporters: Role in macropinocytosis (SLC38A5/SLC38A3) and diet-induced obesity/metabolic syndrome (SLC6A19/SLC6A14/SLC6A6). *Biomolecules* **2022**, *12*, 235.
45. Degirmenci, U.; Wang, M.; Hu, J. Targeting aberrant RAS/RAF/MEK/ERK signaling for cancer therapy. *Cells* **2020**, *9*, 198.
46. Song, Y.;Bi, Z.; Liu, Y.; Qin, F.; Wei, Y.; Wei, X. Targeting RAS-RAF-MEK-ERK signaling pathway in human cancer: Current status in clinical trials. *Genes Dis*. **2023**, *10*, 76-88.
47. Gimple, R.C.; Wang, X. RAS: Striking at the core of the oncogenic circuitry. *Front. Oncol*. **2019**, *9*, 965.
48. Mahauad-Fernandez, W.D.; Felsher, D.W. The Myc and Ras partnership in cancer: Indistinguishable alliance or contextual relationship? *Cancer Res*. **2020**, *80*, 3799-3802.
49. Wise, D.R.; DeBerardinis, R.J.; Mancuso, A.; Sayed, N.; Zhang, X.Y.; Pfeiffer, H.K.; Nissim, I.; Dalkhin, E.; Yudkoff, M.; McMahon, S.B.; Thompson, C.B. Myc regulates a transcriptional program that stimulates mitochondrial glutaminolysis and leads to glutamine addiction. *Proc. Natl. Acad. Sci. USA* **2008**, *105*, 18782-18787.
50. Forcina, G.C.; Dixon, S.J. GPX4 at the crossroads of lipid homeostasis and ferroptosis. *Proteomics* **2019**, *19*, e1800311.
51. Koppula, P.; Zhuang, L.; Gan, B. Cystine transporter SLC7A11/xCT in cancer: Ferroptosis, nutrient dependency, and cancer therapy. *Protein Cell* **2021**, *12*, 599–620.
52. Lee, J.; Roh, J.L. SLC7A11 as a gateway of metabolic perturbation and ferroptosis vulnerability in cancer. *Antioxidants* **2022**, *11*, 2444.
53. Fotiadis, S.; Kanai, Y.; Palacin, M. The SLC3 and SLC7 families of amino acid transporters. *Mol. Aspects Med*. **2013**, *34*, 139-158.

 doi:10.20944/preprints202404.0092.v2

54. Xia, P.; Dubrovska, A. CD98 heavy chain as a prognostic biomarker and target for cancer treatment. *Front. Oncol*. **2023**, *13*, 1251100.
55. Li, Y.; Li, P.K.; Roberts, M.J.; Arend, R.C.; Samant, R.S.; Buchsbaum, D.J. Multi-targeted therapy of cancer by niclosamide: A new application for an old drug. *Cancer Lett.* **2014**, *349*, 8–14.
56. Hamilton, G.; Rath, B. Repurposing of anthelminthics as anticancer drugs. *Oncomedicine* **2018**, *3*, 1–8.
57. Laudisi, F.; Maronek, M.; di Grazia, A.; Monteleone, G.; Stolfi, C. Repositioning of anthelmintic drugs for the treatment of cancers of the digestive system. *Int. J. Mol. Sci.* **2020**, *21*, 4957.
58. Tao, H.; Zhang, Y.; Zeng, X.; Shulman, G.I.; Jin, S. Niclosamide ethanolamine-induced mild mitochondrial uncoupling improves diabetic symptoms in mice. *Nat. Med*. **2014**, *20*, 1263-1269.
59. Kauerova, T.; Perez-Perez, M.J.; Kollar, P. Salicylanilides and their anticancer properties. *Int. J. Mol. Sci*. **2023**, *24*, 1728.
60. Miotto, G.; Rossetto, M.; Di Paolo, M.L.; Orian, L.; Venerando, R.; Roveri, A.; Vuckovic, A.M.; Travain, V.B.; Zaccarin, M.; Zennaro, L.; et al. Insight into the mechanism of ferroptosis inhibition by ferrostatin-1. *Redox Biol*. **2020**, *28*, 101328.
61. Zilka, O.; Shah, R.; Li, B.; Angeli, J.P.F.; Griesser, M.; Conrad, M.; Pratt, D.A. On the mechanism of cytoprotection by ferrostatin-1 and liproxstatin-1 and the role of lipid peroxidation in ferroptotic cell death. *ACS Cent. Sci*. **2017**, *3*, 232
62. Hollestelle, A.; Elstrodt, F.; Nagel, J.H.A.; Kallemeijn, W.W.; Schutte, M. Phosphatidylinositol-3-OH kinase or RAS pathway mutations in human breast cancer cell lines. *Mol. Cancer Res*. **2007**, *5*, 195-201.
63. Kim, R.K.; Suh, Y.; Yoo, K.C.; Cui, Y.H.; Kim, H.; Kim, M.J.; Kim, I.G.; Lee, S.J. Activation of KRAS promotes the mesenchymal features of basal-type breast cancer. *Exp. Mol. Med*. **2015**, *47*, e137.
64. Hui, L.; Zheng, Y.; Yan, Y.; Bargonetti, J.; Foster, D.A. Mutant p53 in MDA-MB-231 breast cancer cells is stabilized by elevated phospholipase D activity and contributes to survival signals generated by phospholipase D. *Oncogene* **2006**, *25*, 7305-7310.
65. Mathew, M.; Nguyen, N.T.; Bhutia, Y.D.; Sivaprakasam, S.; Ganapathy, V. Metabolic signature of Warburg effect in cancer: An effective and obligatory interplay between nutrient transporters and catabolic/anabolic pathways to promote tumor growth. *Cancers (Basel)* **2024**, *16*, 504.
66. Nakanishi, T.; Kekuda, R.; Fei, Y.J.; Hatanaka, T.; Sugawara, M.; Martindale, R.G.; Leibach, F.H.; Prasad, P.D.; Ganapathy, V. Cloning and functional characterization of a new subtype of the amino acid transport system N. *Am. J. Physiol. Cell Physiol*. **2001**, *281*, C1757-C1768.
67. Sniegowski, T.; Korac, K.; Bhutia, Y.D.; Ganapathy, V. SLC6A14 and SLC38A5 drive the glutaminolysis and serine-glycine-one-carbon pathways in cancer. *Pharmaceuticals (Basel)* **2021**, *14*, 216.
68. Shen, X.; Wang, G.; He, H.; Shang, P.; Yan, B.; Wang, X.; Shen, W. SLC38A5 promotes glutamine metabolism and inhibits cisplatin chemosensitivity in breast cancer. *Breast Cancer* **2024**, *31*, 96-104.
69. Sniegowski, T.; Rajasekaran, D.; Sennoune, S.R.; Sunitha, S.; Chen, F.; Fokar, M.; Kshirsagar, S.; Reddy, P.H.; Korac, K.; Mahmud Syed, M.; et al. Amino acid transporter SLC38A5 is a tumor promoter and a novel therapeutic target for pancreatic cancer. *Sci. Rep.* **2023**, *13*, 16863.
70. Kim, M.J.; Kim, H.S.; Kang, H.W.; Lee, D.E.; Hong, W.C.; Kim, J.H.; Kim, M.; Cheong, J.H.; Kim, H.J.; Park, J.S. SLC38A5 modulates ferroptosis to overcome gemcitabine resistance in pancreatic cancer. *Cells* **2023**, *12*, 2509.
71. Girardi, E.; Cesar-Razquin, A.; Lindinger, S.; Papakostas, K.; Konecka, J.; Hemmerich, J.; Kickinger, S.; Kartnig, F.; Gurti, B.; Klavins, K.; et al. A widespread role for SLC transmembrane transporters in resistance to cytotoxic drugs. *Nat. Chem. Biol*. **2020**, *16*, 469-478.
72. Ivanov, A.I. Pharmacological inhibition of endocytic pathways: is it specific enough to be useful? *Methods Mol. Biol*. **2008**, *440*, 15-33.
73. Hassannia, R.; Vandenabeele, P.; Vanden Berghe, T. Targeting ferroptosis to iron out cancer. *Cancer Cell* **2019**, *35*, 830-849.
74. Rodriguez, R.; Schreiber, S.L.; Conrad, M. Persister cancer cells: Iron addiction and vulnerability to ferroptosis. *Mol. Cell* **2022**, *82*, 728-740.
75. Sivaprakasam, S.; Ristic, B.; Mudaliar, N.; Hamood, A.N.; Colmer-Hamood, J.; Wachtel, M.S.; Nevels, A.G.; Kottapalli, K.R.; Ganapathy, V. Hereditary hemochromatosis promotes colitis and colon cancer and causes bacterial dysbiosis in mice. *Biochem. J.* **2020**, *477*, 3867-3883.

 doi:10.20944/preprints202404.0092.v2

76. Figuera-Losada, M.; Thomas, A.G.; Stathis, M.; Stockwell, B.R.; Rojas, C.; Slusher, B.S. Development of a primary microglia screening assay and its use to characterize inhibition of system x_c^- by erastin and its analogs. *Biochem. Biophys. Rep*. **2017**, *9*, 266–272.
77. Zhang, Y.; Tan, H.; Daniels, J.D.; Zandkarimi, F.; Liu, H.; Brown, L.M.; Uchida, K.; O'Conner, O.A.; Stockwell, B.R. Imidazole ketone erastin induces ferroptosis and slows tumor growth in a mouse lymphoma model. *Cell Chem. Biol*. **2019**, *26*, 623-633.e9.
78. Barbosa, E.J.; Lobenberg, R.; Barros de Araujo, G.L.; Bou-Chacra, N.A. Niclosamide repositioning for treating cancer: Challenges and nano-based drug delivery opportunities. *Eur. J. Pharm. Biopharm*. **2019**, *141*, 58–69.
79. Parikh, M.; Liu, C.; Wu, C.Y.; Evans, C.P.; Dall'Era, M.; Robles, D.; Lara, P.N.; Agarwal, N.; Gao, A.C.; Pan, C.X. Phase Ib trial of reformulated niclosamide with abiraterone/prednisone in men with castration-resistant prostate cancer. *Sci. Rep*. **2021**, *11*, 6377.